energies

MDPI

Article

Coordinated Optimal Scheduling of a Ground-Source Heat Pump-Based Hybrid Heating System in a Zero-Carbon Park Under Time-of-Use Tariffs

Long Zhang [1], Sujin Ge [1] and Cheng Yu [2,*]

[1] Shandong Electric Power Engineering Consulting Institute Co., Ltd., Jinan 250013, China
[2] College of Electrical, Energy and Power Engineering, Yangzhou University, Yangzhou 225127, China
* Correspondence: chengyu@yzu.edu.cn

Abstract

This study is based solely on simulations and develops a mixed-integer linear programming (MILP) approach for the coordinated scheduling of a ground-source heat pump, an electric heater, and a thermal storage tank serving office building clusters within a zero-carbon park in a severe cold region under variable heating loads and time-of-use electricity tariffs. Heat source outputs and tank charging and discharging schedules are jointly optimized to minimize operating costs while satisfying hourly heating demand and equipment operating constraints. A case study of office buildings in Daqing compares a baseline strategy without thermal storage, a fixed-window optimization strategy, and a coordinated optimization strategy. Compared with the baseline, coordinated optimization reduces operating costs by 9.22% on the typical day and 12.88% on the extremely cold day. Over the heating season, operating costs decrease from CNY 7.7623 million to CNY 6.9855 million, representing a reduction of 10.01%. Peak-period electricity purchases decrease by 45.83%, whereas total electricity purchases increase by 5.00%. These results indicate that the economic benefits arise primarily from improved electricity-use timing and heat source dispatch, rather than reduced electricity consumption. Sensitivity analysis reveals diminishing returns from increasing tank volume, while the effects of the peak-to-valley electricity price ratio and heat pump charging efficiency on cost savings depend on operating conditions. The findings provide guidance for the cost-effective operation of low-temperature heating systems serving office building clusters in severe cold regions.

Keywords: ground-source heat pump; auxiliary electric heating; thermal storage tank; office building heating; time-of-use tariff; mixed-integer linear programming

Check for updates

Academic Editor: Tapas Mallick

Received: 23 September 2026
Revised: 26 October 2026
Accepted: 29 October 2026
Published: 1 November 2026

Copyright: © 2026 by the authors. Licensee MDPI, Basel, Switzerland. This article is an open access article distributed under the terms and conditions of the Creative Commons Attribution (CC BY) license.

1. Introduction

Zero-carbon parks aim to coordinate clean energy supply and flexible energy use to support the decarbonization of park operations. Within such parks, office-building heating systems must provide reliable heat supply while maintaining economical operation. In severe cold regions, outdoor temperature and building operating schedules shape office heating demand across the season and within each day. For electrically driven heating, the cost of meeting that demand also changes with equipment efficiency and the prevailing electricity tariff. A controller that simply follows the current load may therefore miss opportunities to move electricity use away from expensive hours. Studies of office-building heat pump systems have shown that thermal storage can move part of the heating electricity

demand between hours [1,2]. The scheduling question is how much heat to produce and store at each hour while meeting the building load.

Ground-source heat pumps (GSHPs) draw on low-grade geothermal heat, but the electricity required by the complete plant depends on its configuration and control. In buildings across Jiangsu Province, Zhang et al. [3] found that water pumps and other auxiliary equipment contribute to electricity use alongside the heat pump units. When a second heat source is installed, its response to changing loads and its heating efficiency also affect system operation. In a long-term analysis of a hybrid ground-source and air-source heat pump system, Kaneko and Yoshinaga [4] found that the auxiliary units responded to load fluctuations before the GSHP, reducing the GSHP load factor and causing frequent cycling of the auxiliary units. Zheng et al. [5] compared photovoltaic-assisted GSHP systems with different auxiliary heat sources and found that the lower conversion efficiency of electric heating could compromise economic performance. These findings suggest that auxiliary heat sources can expand the available heating capacity, but their operational value must be assessed in relation to equipment efficiency and heat output allocation.

A storage tank allows some heat to be produced before it is needed, shifting the heat pump's electricity use to another hour. Using a combined design and operation model for residential heating, Renaldi et al. [6] found lower operating costs when storage was scheduled under time-of-use tariffs. Arteconi et al. [7] examined demand-side management in heat pump–storage systems with different heat emitters. Their results showed that stored heat could maintain space heating while the heat pump was switched off during peak periods and improve economic performance under time-of-use tariffs. For GSHP systems, Teamah and Lightstone [8] compared the load-shifting capabilities of water storage and hybrid storage combining water and phase change materials. They found that the storage configuration and operating temperature range affect the required storage volume. In an engineering application, Huang et al. [9] analyzed a treated wastewater-source heat pump system coupled with a large thermal storage pool at a technology park in Beijing, demonstrating the feasibility of shifting heating-related electricity use through off-peak charging. These simulation and operational studies provide a basis for integrating thermal storage with heat pump systems.

The value of stored heat depends on tank capacity and temperature, heat pump performance, and the tariffs faced when heat is produced and used. Lyden and Tuohy [10] varied heat pump and tank sizes and compared the resulting low-price heat production, electricity purchase costs, and capital costs. Using a heat pump–water storage model validated against measured data, Kim and Heo [11] identified a nonlinear relationship between storage capacity and economic performance. Changes in the operating temperature range and tariff structure also affected the economically favorable capacity range. Raising the charging temperature can increase usable storage capacity under certain conditions, but may also increase heat pump electricity demand. Maier et al. [12] compared different air-source heat pump modeling approaches and showed that neglecting the effect of supply temperature on the coefficient of performance (COP) can underestimate storage charging costs and affect the performance of optimized operation. Assessments of storage benefits should therefore account for both usable storage capacity and charging efficiency, without assuming that operating cost savings necessarily imply lower electricity consumption.

Optimization studies have treated heat pump output and tank charging as linked scheduling decisions. For an office building with photovoltaics, a heat pump, thermal storage, and electric vehicles, Liu et al. [13] found that economic model predictive control (MPC) improved operating costs and load shifting relative to rule-based control. Aguilera et al. [14] integrated mixed-integer linear programming (MILP), demand forecasting, and heat pump performance models to schedule large-scale heat pumps and storage in response

to electricity prices and equipment performance. Krützfeldt et al. [15] jointly optimized the sizing and operation of residential heat pump systems using MILP, highlighting the importance of accounting for component interdependencies. For solar-assisted GSHP systems, Weeratunge et al. [16] developed a MILP-based MPC strategy under time-of-use tariffs and showed that integrated thermal storage could improve peak-load shifting and reduce operating costs. Using a different optimization approach, Finck et al. [17] applied dynamic programming to coordinate heat pumps, auxiliary electric heating, and thermal storage in an office building, assessing demand flexibility through energy, power, and cost indicators. The benefits of predictive scheduling also depend on the interaction between control settings and system configuration. D'Ettorre et al. [18] investigated an air-source heat pump–gas boiler system with thermal storage and identified a relationship between the prediction horizon, cost-saving potential, and optimal storage capacity. Lyden and Tuohy [19] compared predictive and fixed-order control across heat pump and hot-water tank configurations, showing that tariff structure and control strategy jointly influence economically favorable system sizing. Beyond simulation-based assessments, Thorsteinsson et al. [20] evaluated price-responsive MPC in an occupied single-family house during a four-month experiment. Their results demonstrated the feasibility of shifting heat pump electricity demand and reducing operating costs, with the achievable savings depending on the selected indoor comfort level. Taken together, these studies support the coordinated optimization of heat production and storage operation, while showing that the resulting benefits depend on equipment constraints, storage characteristics, electricity tariffs, and the information available for scheduling.

In a GSHP–electric heater–tank system, the least-cost schedule depends on the load and on which heat source stored heat can replace. Fixed off-peak charging and peak-period discharging windows may therefore exclude useful operating choices, even when the tariff periods are known. For example, displacing electric heating during intermediate-price periods has a different economic effect from displacing direct heat pump supply during peak-price periods. Storage charging also competes with direct heating for the available heat pump capacity. In addition, storage losses and differences in charging efficiency can cause cost savings and electricity savings to follow different trends. It is therefore necessary to compare fixed-window operation with flexible coordinated scheduling under consistent equipment configurations and storage boundary conditions, considering operating costs, total electricity purchases, and electricity demand during peak-price periods.

Accordingly, this study develops a mixed-integer linear programming (MILP) scheduling model for a ground-source heat pump (GSHP), an auxiliary electric heater, and a water thermal storage tank serving office buildings within a zero-carbon park in Daqing. The model represents the heat balance, equipment capacity limits, storage losses, and operating constraints of the hybrid heating system. Separate coefficients of performance (COPs) are assigned to direct heating and storage charging, and the shared capacity of the heat-pump module bank is considered. Three operating strategies are compared: a baseline strategy without thermal storage (BS), fixed-window optimization (FWO), and coordinated optimization (CO). In the CO strategy, heat-source outputs and tank charging and discharging schedules are determined jointly according to the heating load, electricity price, and available equipment capacity, without prescribing fixed charging and discharging windows. The evaluation covers representative operating conditions, daily scheduling, and aggregated heating-season performance, using operating cost, total electricity purchases, peak-period electricity purchases, and grid power demand as the main indicators. Sensitivity analyses are further conducted to examine the effects of tank volume, the peak-to-valley electricity price ratio, and the heat-pump charging COP. Through this framework, the study

assesses the operating value of coordinated scheduling for hybrid heating systems in severe cold regions.

2. System Configuration and Heating Load

2.1. System Configuration and Heat Supply Boundaries

Figure 1 shows the GSHP and an electric resistance boiler connected to both the building heating circuit and a thermal storage tank. The GSHP can meet demand directly or use capacity remaining after direct supply to charge the tank. Auxiliary heating is provided by an electric resistance boiler, which can either supplement the direct heat supply or charge the tank. For each heat source, the direct-heating and storage-charging branches share the available equipment capacity, and their outputs are jointly determined by the scheduling model. The tank releases heat to the heating circuit through a separate heat-exchange branch, allowing heat production and building heat use to be separated in time. Under time-of-use tariffs, the system can produce and store heat at a lower cost in advance, then use the stored heat to displace more expensive heat production later. However, the operating modes impose different constraints on heat pump charging efficiency, available output, and tank state. A lower electricity price therefore does not necessarily make storage charging economical for every heat source. Heat source dispatch and tank charging and discharging schedules must be determined jointly. Using known heating loads as inputs, the model optimizes the hourly outputs of the GSHP, electric heater, and storage tank within each 24 h period. The schedule must satisfy the hourly heat balance and restore the initial storage state by the end of the day. Building heating demand is held constant across the strategies; cost savings are not obtained by lowering indoor temperature setpoints or curtailing the heating load.

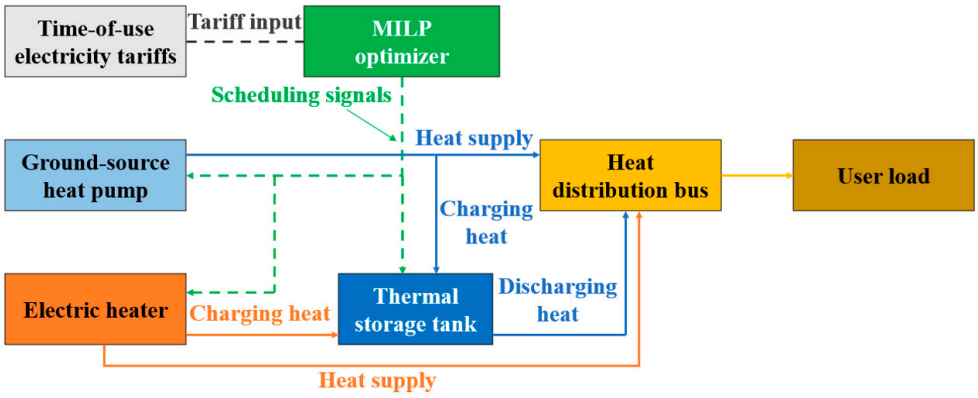


Figure 1. Schematic of the GSHP–electric heater–thermal storage system.

2.2. Building Characteristics and Heating Loads

The case study considers office buildings within a zero-carbon park in Daqing, Heilongjiang Province, a representative northern Chinese city with a severe cold climate. Measured hourly outdoor dry-bulb temperatures in Daqing are used as the meteorological boundary conditions for system operation. These measured temperatures range from −29.633 °C to 14.967 °C. The minimum value of −29.633 °C characterizes the extreme outdoor condition in the case-study dataset. For an indoor reference temperature of 20 °C, the corresponding indoor–outdoor temperature difference is $\Delta T = 49.633$ K. This study is simulation-based and does not include a physical experiment or field test. Hourly heating loads are generated using an EnergyPlus building model, while measured hourly outdoor dry-bulb temperatures are used as meteorological boundary conditions. The building characteristics and load calculation inputs are summarized in Table 1. The total office floor

area is 800,000 m^2, the window-to-wall ratio is 0.50, the floor area per occupant is 12 m^2, and the design heating load for mechanical ventilation is 25 W/m^2. The indoor temperature is set to 20 °C during working hours, from 08:00 to 17:00, and reduced to a 12 °C setback for frost-protection heating outside these hours. Mechanical ventilation is provided, and the heating load calculation accounts for outdoor-air heating demand, internal heat gains from occupants, lighting, and equipment, and solar heat gains [21,22].

Table 1. Building model parameters.

Item	Value
Building type	Office building
Total floor area (m^2)	800,000
Window-to-wall ratio	0.50
Floor area per occupant (m^2/person)	12
Design heating load for mechanical ventilation (W/m^2)	25
Total occupant heat gain density (W/m^2)	9.0
Lighting heat gain density (W/m^2)	16
Office-equipment heat gain density (W/m^2)	10.8
External-wall thermal transmittance ($W/(m^2 \cdot K)$)	0.35
Window thermal transmittance ($W/(m^2 \cdot K)$)	1.70
Roof thermal transmittance ($W/(m^2 \cdot K)$)	0.25
Indoor temperature setpoints: working/non-working hours (°C)	20/12
Normal heating hours on weekdays	08:00–17:00

Figure 2 presents the daily mean heating load and outdoor temperature over the heating season. As shown in Figure 2a, the heating load is generally lower at the beginning and end of the season and higher during the middle. The load gradually increases as the heating season progresses, exhibits several local peaks during midwinter, and subsequently declines. Pronounced day-to-day fluctuations are superimposed on this seasonal pattern, indicating substantial differences in the required heat supply between days. In Figure 2b, the daily mean outdoor temperature initially decreases and then rises again. Relatively high temperatures at the beginning of the season are followed by a sustained cold period in midwinter and gradual warming toward the end. Short-term alternations between colder and warmer conditions occur during both the cooling and warming phases, requiring the heating system to accommodate daily weather fluctuations as well as seasonal changes.

Taken together, Figure 2a,b show that the daily mean heating load and outdoor temperature are generally inversely related, with higher loads concentrated in colder periods. As the outdoor temperature decreases, the indoor–outdoor temperature difference increases, raising heat transmission losses through the building envelope and the heating demand associated with ventilation air. Building heating demand consequently increases. These heat requirements decrease as the outdoor temperature rises. However, the two curves do not mirror each other exactly because the net heating load also depends on building operating schedules, indoor temperature setpoints, and heat gains from occupants, lighting, equipment, and solar radiation. Outdoor temperature is therefore an important driver of seasonal load variations, while building operation and heat gains further influence day-to-day differences.

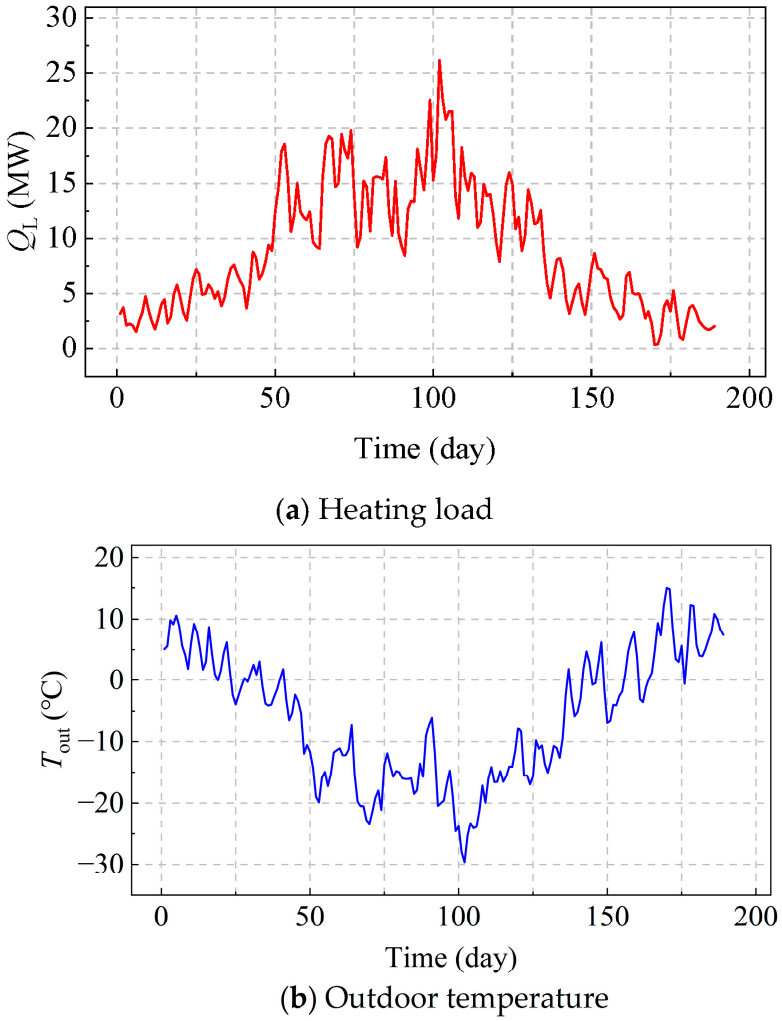


Figure 2. Daily mean heating load and outdoor temperature over the heating season.

3. Mathematical Model

3.1. Ground-Source Heat Pump Model

Different supply water temperatures are used for direct heating and tank charging. The corresponding coefficients of performance (COPs) are specified separately before optimization [23]. The index t denotes the hourly scheduling interval, with $t = 1, \ldots, 24$. The equipment subscripts h, e and s denote the heat pump, electric heater, and storage tank, respectively, while the branch subscripts d and c denote direct heating and charging. The variables Q, P, and E represent thermal power, electrical power, and stored thermal energy, respectively. The total heat pump electrical power is given by

$$P_{\mathrm{h}}(t) = \frac{Q_{\mathrm{hd}}(t)}{\mathrm{COP_d}} + \frac{Q_{\mathrm{hc}}(t)}{\mathrm{COP_c}} \tag{1}$$

where $P_{\mathrm{h}}(t)$ is the total electrical power consumed by the heat pump; $Q_{\mathrm{hd}}(t)$ and $Q_{\mathrm{hc}}(t)$ are its thermal outputs for direct heating and tank charging, respectively. The coefficients $\mathrm{COP_d}$ and $\mathrm{COP_c}$ correspond to direct heating and charging and are treated as known constants within each optimization process. A $\mathrm{COP_d}$ of 3.5 is used for direct heating at 45 °C, and a $\mathrm{COP_c}$ of 2.5 is used for charging at 60 °C.

The two operating modes use the same heat pump module bank, and their outputs satisfy the following shared-capacity constraint:

$$\begin{aligned} &\frac{Q_{\mathrm{hd}}(t)}{\overline{Q}_{\mathrm{hd}}} + \frac{Q_{\mathrm{hc}}(t)}{\overline{Q}_{\mathrm{hc}}} \le 1 \\ &0 \le Q_{\mathrm{hd}}(t) \le \overline{Q}_{\mathrm{hd}}, 0 \le Q_{\mathrm{hc}}(t) \le \overline{Q}_{\mathrm{hc}} \end{aligned} \tag{2}$$

where $\overline{Q}_{\mathrm{hd}}$ and $\overline{Q}_{\mathrm{hc}}$ are the rated heating capacities for direct heating and charging, respectively, set to 22.40 MW and 20.16 MW. This constraint represents the allocation of the module bank capacity between the two operating modes.

3.2. Auxiliary Electric Heater Model

The auxiliary electric heater is modeled using a constant electricity-to-heat conversion efficiency. The electrical powers of the direct-heating and charging branches are nonnegative and share the rated electrical capacity:

$$\begin{aligned} &Q_{\mathrm{ed}}(t) = \eta_{\mathrm{e}} P_{\mathrm{ed}}(t), Q_{\mathrm{ec}}(t) = \eta_{\mathrm{e}} P_{\mathrm{ec}}(t) \\ &0 \le P_{\mathrm{ed}}(t) + P_{\mathrm{ec}}(t) \le \overline{P}_{\mathrm{e}} \end{aligned} \tag{3}$$

where $P_{\mathrm{ed}}(t)$ and $P_{\mathrm{ec}}(t)$ are the electrical powers used for direct heating and charging, respectively; $Q_{\mathrm{ed}}(t)$ and $Q_{\mathrm{ec}}(t)$ are the corresponding thermal outputs. The conversion efficiency η_{e} is set to 0.98, and the rated electrical power $\overline{P}_{\mathrm{e}}$ is 25.60 MW. The electric heater can meet an immediate heat supply shortfall or contribute to intertemporal heat supply by charging the tank. The operating periods and power outputs of both branches are determined by the optimization model.

3.3. Thermal Storage Tank Model

The thermal storage tank is represented by a well-mixed lumped-parameter model, with the bulk water temperature describing its thermal state. The building supply and return water temperatures are 45 °C and 35 °C, respectively, and the tank is charged and discharged through a dedicated heat exchanger. With minimum approach temperature differences of 2 K during discharging and 3 K during charging, a reference tank temperature range of 47–57 °C is adopted. The heat pump supply water temperature during charging is 60 °C. Taking the lower reference temperature as the zero-energy reference, the tank heat capacity, nominal storage capacity, and bulk water temperature are related by

$$C_{\mathrm{w}} = \frac{\rho c_{\mathrm{p}} V}{3600}, E_{\mathrm{n}} = C_{\mathrm{w}}(T_{\max} - T_{\min}), T(t) = T_{\min} + \frac{E(t)}{C_{\mathrm{w}}} \tag{4}$$

where C_{w} is the thermal capacitance of the tank water (kWh/K); ρ is the water density, set to 1000 kg/m^3; c_{p} is the specific heat capacity of water, set to 4.18 kJ/(kg·K); and V is the tank volume (m^3); The nominal thermal storage capacity is denoted by E_{n}, kWh; The temperatures $T_{\min}$ and $T_{\max}$ are the lower and upper bounds of the reference temperature range (°C); The variables $E(t)$ and $T(t)$ denote the stored thermal energy and water temperature at the end of interval t, respectively. The state of charge (SOC) is defined as

$$\mathrm{SOC}(t) = \frac{E(t)}{E_{\mathrm{n}}} = \frac{T(t) - T_{\min}}{T_{\max} - T_{\min}} \tag{5}$$

The tank volume is 2880 m^3, corresponding to a thermal capacitance of 3344 kWh/K and a nominal storage capacity E_{n} of 33.44 MWh. The lower and upper SOC limits, $\mathrm{SOC}_{\min}$ and $\mathrm{SOC}_{\max}$, are set to 0.10 and 0.90, respectively. The usable thermal storage capacity available for scheduling, E_{u}, is therefore

$$E_{\mathrm{u}} = (\mathrm{SOC}_{\max} - \mathrm{SOC}_{\min}) E_{\mathrm{n}} \tag{6}$$

The resulting operating temperature range is 48–56 °C. Both the initial and end-of-day SOC values are set to 0.50, corresponding to a water temperature of 52 °C. The minimum water temperature satisfies the heat-transfer requirement on the building supply side, while the maximum remains below the heat pump charging supply temperature with an adequate temperature difference. The usable storage capacity is thus determined jointly by the 47–57 °C reference range and the SOC limits, corresponding to the actual operating range of 48–56 °C.

Tank charging power comprises contributions from the heat pump and electric heater:

$$Q_{\mathrm{ch}}(t) = Q_{\mathrm{hc}}(t) + \eta_{\mathrm{e}} P_{\mathrm{ec}}(t) \tag{7}$$

Charging and discharging process losses and tank-to-ambient standby heat losses are modeled separately. Standby heat losses are evaluated using the tank temperature at the beginning of each time step. The discrete storage energy balance is

$$\begin{aligned} E(t) &= \left(1 - \tfrac{UA\Delta t}{C_{\mathrm{w}}}\right) E(t-1) + \eta_{\mathrm{ch}} Q_{\mathrm{ch}}(t)\Delta t - \tfrac{Q_{\mathrm{dis}}(t)\Delta t}{\eta_{\mathrm{dis}}} - UA\Delta T_{\mathrm{min}}\Delta t \\ \Delta T_{\mathrm{min}} &= T_{\mathrm{min}} - T_a \end{aligned} \tag{8}$$

where $Q_{\mathrm{ch}}(t)$ is the thermal power entering the tank charging branch, and $Q_{\mathrm{dis}}(t)$ is the thermal power delivered from the tank to the heating circuit. Δt denotes the scheduling time-step duration, while $\Delta T_{\mathrm{min}} = T_{\mathrm{min}} - T_a$ denotes the temperature difference between the minimum reference tank temperature and the equipment-room ambient temperature. The charging and discharging efficiencies, η_{ch} and η_{dis}, are both set to 0.95. The overall thermal conductance UA, defined as the product of the overall heat transfer coefficient and heat transfer area, is set to 1.0 kW/K. The equipment-room ambient temperature T_{a} is 20 °C. The charging and discharging efficiencies, η_{ch} and η_{dis}, represent the effective process efficiencies of heat transfer into and out of the thermal storage tank, respectively. They account for irreversible losses associated with the charging and discharging processes that are not explicitly resolved in the lumped-parameter model. These process losses are distinct from standby heat loss to the equipment-room ambient, which is calculated separately through the UA terms.

The tank is also subject to storage energy bounds and an end-of-day restoration constraint:

$$\begin{aligned} &\mathrm{SOC}_{\mathrm{min}} E_{\mathrm{n}} \le E(t) \le \mathrm{SOC}_{\mathrm{max}} E_{\mathrm{n}} \\ &E(24) = E(0) = \mathrm{SOC}(0) E_{\mathrm{n}} \end{aligned} \tag{9}$$

where $E(0)$ and $E(24)$ are the initial and end-of-day stored thermal energies, respectively, and $\mathrm{SOC}(0)$ is the initial state of charge, set to 0.50. Restoring the initial stored energy at the end of the day ensures that the strategies are compared under the same thermal reserve conditions and that the cost of restoring the stored heat is included in the scheduling results. Standby heat losses are included for strategies that use the tank. Under BS, the tank is isolated, and its heat losses are excluded from the operating energy balance.

3.4. Heat Balance and Operating Constraints

In each time instant, direct heat pump supply, direct electric heating, and tank discharge jointly meet the building heating load:

$$Q_{\mathrm{hd}}(t) + \eta_{\mathrm{e}} P_{\mathrm{ed}}(t) + Q_{\mathrm{dis}}(t) = Q_{\mathrm{L}}(t) \tag{10}$$

where $Q_{\mathrm{L}}(t)$ is the building heating load during time instant t, kW. Heat supplied to the tank contributes to subsequent heat delivery through the storage energy balance and is not counted again as heat supplied directly to the building in the current interval.

Tank charging and discharging powers are limited by the heat-exchange equipment capacities. Binary variables are introduced to prevent simultaneous charging and discharging within the same interval:

$$0 \le Q_{\mathrm{ch}}(t) \le \overline{Q}_{\mathrm{ch}} u_{\mathrm{ch}}(t), 0 \le Q_{\mathrm{dis}}(t) \le \overline{Q}_{\mathrm{dis}} u_{\mathrm{dis}}(t) \tag{11}$$

$$u_{\mathrm{ch}}(t) + u_{\mathrm{dis}}(t) \le 1, u_{\mathrm{ch}}(t), u_{\mathrm{dis}}(t) \in \{0,1\} \tag{12}$$

where $u_{\mathrm{ch}}(t)$ and $u_{\mathrm{dis}}(t)$ are binary variables enabling the charging and discharging modes, respectively. The maximum charging and discharging powers, $\overline{Q}_{\mathrm{ch}}$ and $\overline{Q}_{\mathrm{dis}}$, are set to 28.80 MW and 25.60 MW. A binary value of 1 permits the corresponding mode to operate, while its power remains subject to optimization within the specified limit. A value of 0 forces the power of that mode to zero.

The total grid power drawn by the heat sources is constrained by the grid connection capacity:

$$P_{\mathrm{g}}(t) = \frac{Q_{\mathrm{hd}}(t)}{\mathrm{COP}_{\mathrm{d}}} + \frac{Q_{\mathrm{hc}}(t)}{\mathrm{COP}_{\mathrm{c}}} + P_{\mathrm{ed}}(t) + P_{\mathrm{ec}}(t) \le \overline{P}_{\mathrm{g}} \tag{13}$$

where $P_{\mathrm{g}}(t)$ is the total grid power drawn by the heat pump and electric heater, and $\overline{P}_{\mathrm{g}}$ is the grid import power limit for the heating equipment.

3.5. Objective Function and Solution Method

The objective is to minimize the total system operating cost over a 24 h scheduling horizon. This cost comprises electricity purchase costs and variable operation and maintenance (O&M) costs:

$$\min C = C_{\mathrm{el}} + C_{\mathrm{om}} \tag{14}$$

where C is the daily system operating cost, C_{el} is the daily electricity purchase cost, and C_{om} is the daily variable operation and maintenance cost. Electricity purchase costs are calculated from the electricity consumed by the heat pump and electric heater in each interval and the corresponding time-of-use electricity price. Variable O&M costs comprise contributions from the heat pump, electric heater, and storage tank. Heat pump and electric heater O&M costs are calculated based on their respective heat production, while tank O&M costs are based on the sum of charging and discharging heat throughput.

Mixed-integer linear programming (MILP) can jointly optimize continuous equipment outputs and discrete operating modes. In this study, branch powers and stored thermal energy are defined as continuous variables. Binary variables indicate whether tank charging or discharging is permitted, preventing both modes from operating simultaneously within the same interval. Since equipment capacities, heat pump COPs, and efficiency parameters are specified before optimization, the objective function and constraints remain linear. The resulting MILP model jointly determines the tank operating mode and equipment outputs. The model is solved using a branch-and-bound-based method. First, the binary restrictions are relaxed, and the corresponding linear programming problem is solved to obtain a lower bound on operating costs. Branches are then created for variables that do not satisfy the integrality requirements. Infeasible branches and those that cannot improve the current best solution are progressively eliminated. During the search, feasible integer solutions are used to update the upper bound, while the gap between the upper and lower bounds is narrowed. Once the optimality gap satisfies the prescribed tolerance, a scheduling solution meeting the required level of optimality is obtained.

The MATLAB R2023a solver intlinprog is used, with the relative optimality gap tolerance set to 10^{-6}. A 24 h scheduling model with a 1 h time step is constructed using the hourly heating load, time-of-use electricity prices, and equipment parameters as inputs. The initial and end-of-day storage states are constrained to be equal. After each solution, the

solver status, optimality gap, and constraint satisfaction are checked, and the heat source outputs, tank storage states, and grid power demand are extracted. Each day of the heating season is optimized independently. Daily operating costs and electricity purchases are then aggregated to evaluate the heating-season performance of the different strategies.

The checks described above verify the mathematical implementation and numerical feasibility of the scheduling model. However, because no measured equipment-operation data or independent experimental case are available, the present study does not provide empirical validation of the model. The BS, FWO, and CO cases are used for comparative scheduling analysis under identical system inputs, but they should not be regarded as external validation benchmarks. Future work will use pilot-building measurements to calibrate and validate the component models by comparing predicted and measured heating loads, COP, tank SOC, electricity consumption, peak power, and operating costs.

In practice, the CO strategy can be implemented as a supervisory scheduling layer integrated with the building management system. It requires forecasts of hourly heating loads and outdoor temperatures, time-of-use electricity prices, equipment operating limits, and the initial tank SOC to determine set points for the GSHP, electric heater, pumps, and control valves. Measurements of outdoor and supply/return water temperatures, equipment power, and tank temperature or SOC support state updating and feedback correction. When suitable sensing and control interfaces are already available, the additional implementation mainly involves the optimization algorithm and communication functions, thereby limiting the added control complexity.

4. Case Study Setup and Performance Indicators

4.1. Time-of-Use Tariffs and Comparison Strategies

The time-of-use electricity tariffs are listed in Table 2 and comprise peak, intermediate-price, and off-peak periods. The baseline peak-to-valley price ratio is 2.61. Each hour is assigned the electricity price of the corresponding tariff period. The tariff schedule is used as a case-study input to examine how equipment dispatch responds to price signals.

Table 2. Time-of-use electricity tariffs.

Period	Time Intervals	Price (CNY/kWh)
Peak	07:00–11:00, 16:00–20:00	0.86
Intermediate	06:00–07:00, 11:00–12:00, 14:00–16:00, 20:00–24:00	0.60
Off-peak	00:00–06:00, 12:00–14:00	0.33

As summarized in Table 3, three strategies are compared: the baseline strategy (BS), fixed-window optimization (FWO), and coordinated optimization (CO). Under BS, the thermal storage tank remains inactive, and hourly heating demand is met by prioritizing direct heat pump supply. The electric heater covers the portion of the load that exceeds the heat pump capacity. FWO activates the storage tank but permits charging only during off-peak periods and discharging only during peak periods. Heat source outputs and tank charging and discharging powers are optimized within these predefined windows. The restrictions therefore apply to the allowable operating periods rather than prescribing fixed equipment power outputs. CO removes the predefined charging and discharging windows while retaining the same equipment and storage-state constraints. It jointly determines branch outputs and tank operating schedules according to the heating load, electricity prices, and available heat source capacity.

Table 3. Overview of the scheduling strategies.

Strategy	Operating Rule	Tank State Requirement
BS	No storage; GSHP prioritized, with electric heating covering the remaining load	Tank inactive
FWO	Off-peak charging and peak-period discharging only; dispatch optimized within these windows	Initial and end-of-day SOC both 0.50
CO	No predefined charging/discharging windows; branch outputs jointly optimized	Initial and end-of-day SOC both 0.50

All three strategies use the same heating loads, electricity tariffs, heat source capacities, and grid import power limit. FWO and CO also use identical tank capacities and charging and discharging parameters. Their initial and end-of-day SOC values are both fixed at 0.50, preventing additional benefits from being attributed to net depletion of the initial stored heat. The comparison between BS and FWO evaluates the operational improvement obtained by introducing thermal storage under fixed-window operation. The comparison between FWO and CO then identifies the additional economic benefits of relaxing the charging and discharging time restrictions.

4.2. Parameters and Representative Inputs

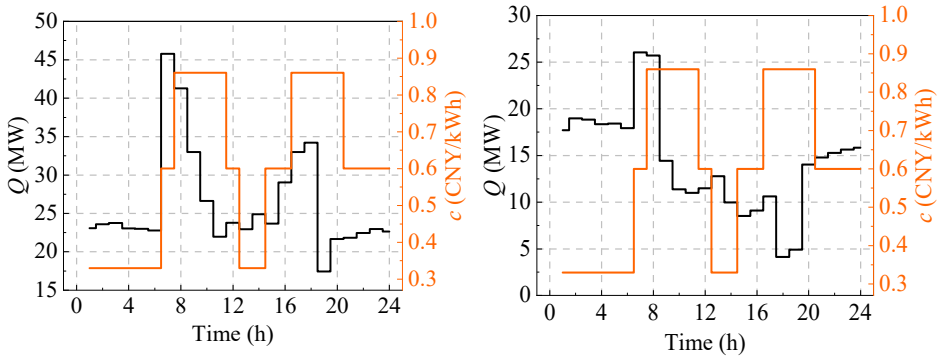
The main equipment and operating parameters are listed in Table 4. To represent a feasible and representative configuration for the 800,000 m^2 office-building case, the GSHP direct-heating capacity, GSHP storage-charging capacity, electric-heater rating, and tank volume were set to 22.40 MW, 20.16 MW, 25.60 MW, and 2880 m^3, respectively. Direct heating and storage charging share the heat-pump module-bank capacity; therefore, their rated heating capacities should not be added together. The lower rated capacity and COP assigned to the charging mode account for the performance degradation associated with the higher charging supply-water temperature. The electric-heater capacity was specified to cover the residual heating demand when the available direct-heating capacity of the GSHP is insufficient and to support tank charging when spare GSHP capacity is unavailable. The tank volume corresponds to a nominal storage capacity of 33.44 MWh and a usable storage capacity of 26.752 MWh after applying the SOC limits. The tank operating temperature range is compatible with both the building supply temperature and the heat-pump charging temperature. These equipment characteristics were treated as fixed case-study inputs; the present study optimizes operating schedules without jointly optimizing the installed capacities.

These equipment characteristics were treated as fixed case-study inputs; the present study optimizes operating schedules without jointly optimizing the installed capacities. The MILP formulation can be applied to other building scales and types by recalibrating the heating-load profiles, occupancy schedules, envelope and internal-gain assumptions, equipment capacities, storage parameters, and electricity tariffs. However, its transferability to other commercial and residential buildings requires further case studies.

Table 4. Equipment and operating parameters.

Parameter	Value
GSHP rated heating capacity: direct heating (MW)	22.40
GSHP rated heating capacity: tank charging (MW)	20.16
GSHP COP: direct heating/charging	3.5/2.5
GSHP supply water temperature: direct heating/charging (°C)	45/60
Building supply/return water temperature (°C)	45/35
Electric heater rated electrical power (MW)	25.60
Tank volume (m^3)	2880
Tank reference temperature range (°C)	47–57
Tank operating temperature range (°C)	48–56
Nominal thermal storage capacity (MWh)	33.44
Minimum, maximum, and initial/final SOC	0.10, 0.90, 0.50
Maximum tank charging/discharging thermal power (MW)	28.80, 25.60
Variable O&M rates: GSHP/electric heater (CNY/kWh)	0.015, 0.005
Tank throughput-based variable O&M rate (CNY/kWh)	0.003
Grid import power limit for heating equipment (MW)	32.00

Figure 3 shows the hourly heating loads (black lines) and time-of-use electricity prices (orange lines) for the extremely cold day and the typical day. In Figure 3a, the extremely cold day has a relatively high overall load, with a sharp morning increase followed by a decline and a second increase in the afternoon. The morning peak substantially exceeds the rated direct-heating capacity of the heat pump, requiring supplementary heat from the electric heater or storage tank. The high base load also occupies most of the heat pump capacity, leaving limited capacity for charging after the current heating demand has been served. In Figure 3b, the typical day has a lower overall load but still exhibits a pronounced morning peak. A lower seasonal demand level therefore does not eliminate short-duration heat supply shortfalls. The relatively low nighttime and midday loads leave some spare heat pump capacity for charging after direct heating demand is met. Heat can thus be stored in advance to alleviate subsequent demand peaks. The two operating conditions differ not only in total heating demand but also in the heat source capacity available for storage charging. The higher morning loads partly overlap with peak-price periods, increasing the cost pressure associated with direct heating, whereas nighttime and midday off-peak periods provide opportunities for lower-cost charging. However, load changes and tariff transitions are not fully synchronized, and current heating demand must still be met during low-price periods. Storage schedules must therefore account for available heat source capacity and subsequent heating needs, rather than being determined by electricity prices alone.



(**a**) Extremely cold day (**b**) Typical day

Figure 3. Hourly heating loads and time-of-use electricity prices.

4.3. Performance Metrics

Economic performance is evaluated using the operating cost saving rate, with BS serving as the reference under the same operating conditions:

$$R_c = \frac{C_{BS} - C_s}{C_{BS}} \times 100\% \tag{15}$$

where R_c is the cost saving rate (%); C_{BS} is the operating cost of BS; and C_s is the operating cost of the strategy being evaluated. The heating-season cost saving rate is calculated from the aggregated operating costs over the entire heating season. Cumulative cost savings are obtained by summing the daily cost differences relative to BS.

Total electricity purchases, peak-period electricity purchases, and maximum grid import power are also evaluated to distinguish changes in operating costs, electricity consumption, and power demand. Total electricity purchases are calculated by summing the product of grid import power and the time-step duration over all intervals. The indicators for peak-price periods are defined as:

$$\begin{aligned} W_p &= \sum_{t \in \Omega_p} P_g(t) \Delta t \\ P_p &= \max_{t \in \Omega_p} P_g(t) \end{aligned} \tag{16}$$

where Ω_p denotes the set of peak-price intervals specified in Table 2; W_p is the electricity purchased during these intervals (kWh); and P_p is the maximum grid import power during peak-price periods (kW).

5. Results and Discussion

5.1. Heat Source Dispatch

Table 5 compares the operating results of the three strategies for the extremely cold day and the typical day. In both cases, BS incurs the highest operating cost, followed by FWO and CO. This ordering shows that introducing thermal storage and optimizing equipment operating schedules can improve system economics. Relative to BS, CO reduces operating costs by 12.88% on the extremely cold day and 9.22% on the typical day. The corresponding reductions relative to FWO are 2.33% and 2.16%, respectively. These results indicate that removing predefined charging and discharging windows provides additional operating flexibility under the same equipment capacity and storage-state constraints. Fixed-window operation does not exploit all the cost-saving opportunities available under these conditions.

Table 5. Operating results for representative days.

Day Type	Strategy	Cost (10^4 CNY)	Cost Savings (%) *	Total Electricity (MWh)	Peak-Period Electricity (MWh)
Extremely cold day	BS	17.072	0.00	250.85	106.61
	FWO	15.228	10.80	255.83	68.21
	CO	14.873	12.88	253.18	60.15
Typical day	BS	6.496	0.00	103.87	29.90
	FWO	6.027	7.22	106.50	18.87
	CO	5.897	9.22	103.83	19.91

* Cost savings are calculated relative to BS.

Both FWO and CO reduce peak-period electricity purchases in the two cases, but the reduction in operating costs is not accompanied by a substantial decrease in total electricity purchases. Under CO, total electricity purchases increase slightly on the extremely cold day and remain approximately equal to those of BS on the typical day. Improved economic performance should therefore not be interpreted directly as an energy-saving benefit. On the typical day, FWO purchases less electricity during peak periods than CO but incurs a higher operating cost. Peak-period electricity purchases alone are thus insufficient to assess scheduling economics. The full-day distribution of electricity use and the heating cost in each period must be considered, rather than simply minimizing electricity purchases during peak periods.

Figure 4 presents heat source dispatch under CO for the extremely cold day and the typical day. Above zero, direct heat pump supply, direct electric heating, and tank discharge jointly meet the building heating load. Heat pump and electric heater charging powers are plotted below zero.

As shown in Figure 4a, direct heat pump output remains high during most hours of the extremely cold day. When the morning load rises rapidly, supplementary heat from both the electric heater and the storage tank is still required. Current heating demand occupies most of the heat pump capacity, leaving little spare capacity for tank charging. Charging is therefore provided mainly by the electric heater. The system stores heat during the lower-price nighttime and midday periods and releases it during the higher-load morning and afternoon periods, reducing the need for direct electric heating at those times. In this case, the economic value of electric charging arises primarily from shifting electricity use between periods, rather than improving electricity-to-heat conversion efficiency. The electric heater must still cover the heating shortfall that cannot be met by stored heat, so the tank does not completely replace the auxiliary heat source.

In Figure 4b, the lower nighttime and midday loads on the typical day leave spare heat pump capacity after direct heating demand has been met. The tank is consequently charged mainly with heat produced by the heat pump. When the morning load increases, discharging the tank allows heat produced earlier using spare heat pump capacity to meet subsequent demand. This bridges the gap between the instantaneous direct-heating capacity of the heat pump and the building load, eliminating the need for direct electric heating in this case. Compared with the extremely cold day, this operating pathway changes the heat source serving part of the load as well as the timing of electricity use. Although the heat pump COP is lower during charging than during direct heating, and storage introduces charging and discharging losses, replacing part of the electric heating demand with heat pump output can offset some of the additional electricity requirement. Changes in total electricity use therefore cannot be inferred from storage losses alone.

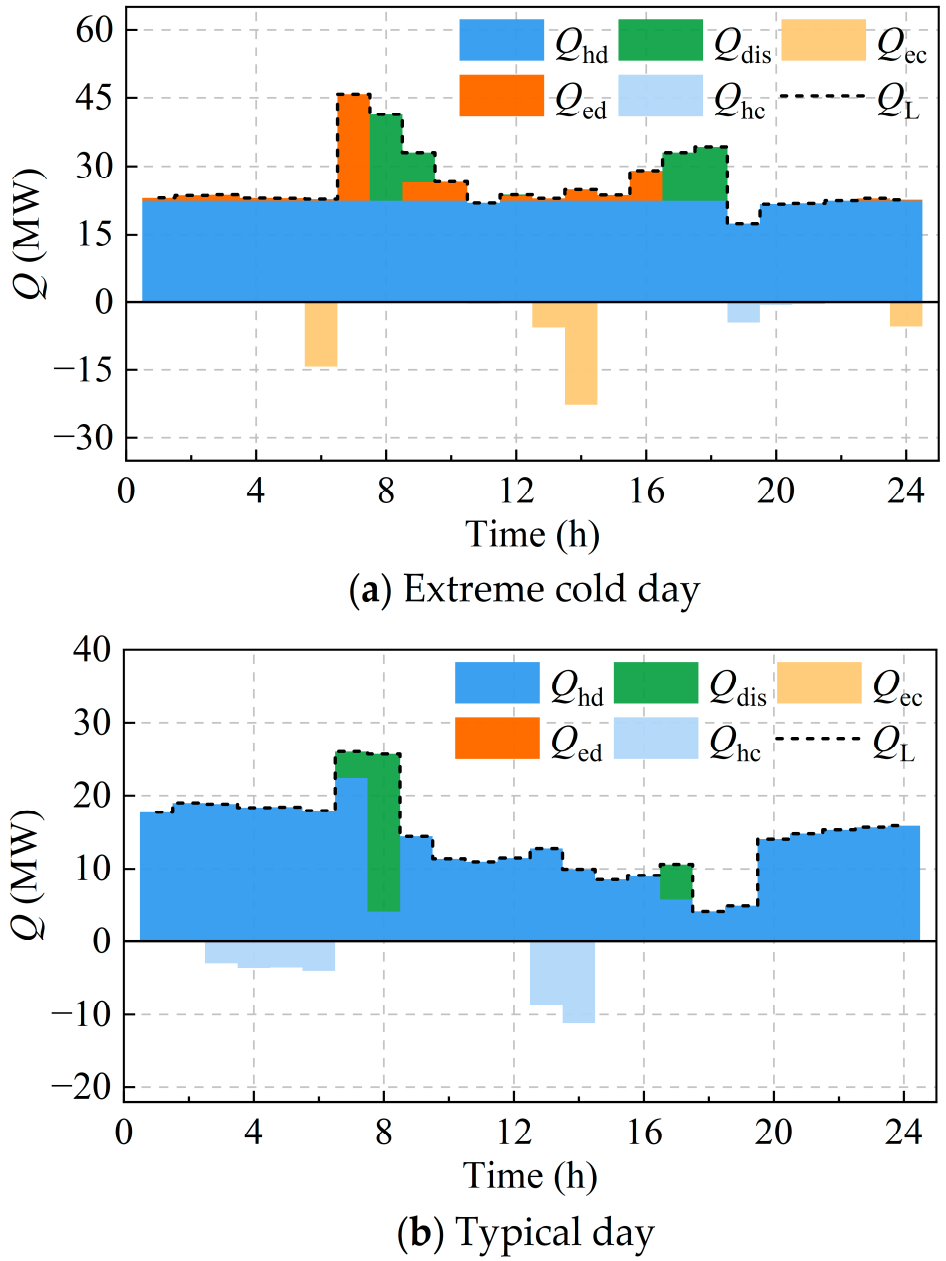
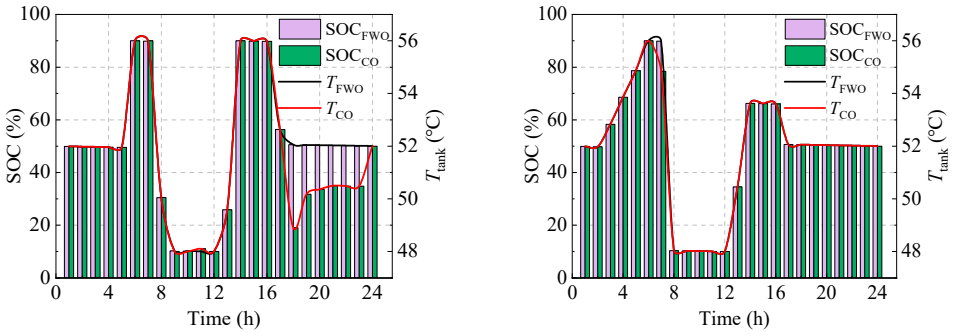


Figure 4. MILP-based coordinated heat dispatch.

On the typical day, the tank also discharges during the morning intermediate-price period, illustrating the flexibility of CO in allocating stored heat. The value of stored heat depends on the cost of the heat supply it displaces, which is determined by both electricity prices and heat source efficiency. Under the parameter values used in this study, electric heating during intermediate-price periods remains more expensive per unit of heat than direct heat pump supply during peak periods. Allocating some stored heat to reduce intermediate-period electric heating may therefore be more economical than reserving all of it for peak-period discharge. Across the two cases, spare heat pump capacity determines the available charging pathways, while subsequent heating costs influence the allocation of stored heat. CO coordinates these two aspects so that limited equipment capacity and stored energy are used preferentially to reduce high-cost heat supply.

5.2. Storage State and Grid Power Demand

In both cases in Figure 5, charging precedes the morning load rise, and SOC falls as the tank supplies heat. The extremely cold day has a second midday charge to near the SOC ceiling, followed by another discharge. On the typical day, the second charging period occurs in the early afternoon and raises SOC to only about 65%. The amount of heat stored during the second charging period is therefore not determined by tank capacity alone, but also by spare heat pump capacity, charging costs, and subsequent heating demand. Fully charging the tank during every cycle is not necessarily the preferred operating choice. Tank temperature follows SOC because of their linear relationship and remains within the prescribed range of 48–56 °C.



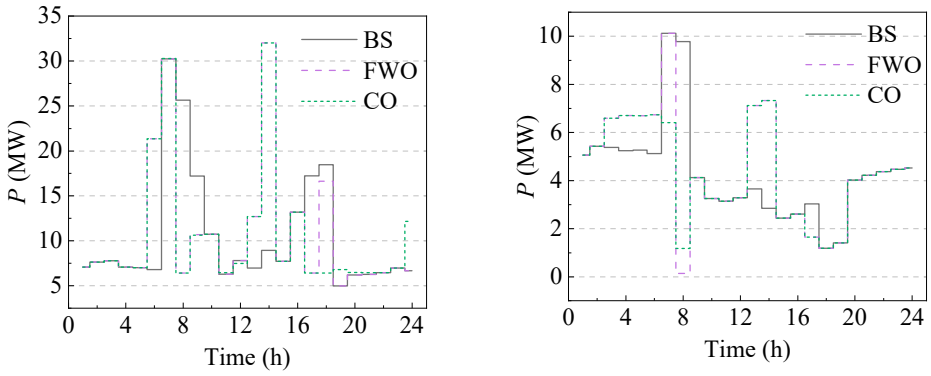
(**a**) Extremely cold day (**b**) Typical day

Figure 5. Tank SOC and temperature.

During the afternoon of the extremely cold day, the SOC under CO is markedly lower than under FWO. This difference reflects the combined effects of charging windows and the end-of-day storage constraint. Since FWO permits charging only within the specified off-peak windows, it must account in advance for the terminal storage requirement, limiting the heat available for later discharge. CO permits recharging outside these fixed windows, allowing more stored heat to be released first and the terminal state to be restored according to subsequent operating conditions. This increases the flexibility of heat allocation and reduces the duration of high-temperature storage during certain periods, lowering the associated standby heat losses. Both strategies begin and end the day at an SOC of 50%, ensuring that the comparison does not depend on an end-of-day storage deficit.

In Figure 6a, activating the tank reduces grid power demand during the morning and afternoon high-price periods of the extremely cold day, but creates new power peaks during charging. CO reaches the 32 MW grid import limit during the midday off-peak period, exceeding the maximum daily grid power demand under BS. Under this high-load condition, spare heat pump capacity is limited, and tank charging relies mainly on electric heating. Charging electricity demand is added to the electricity required for current direct heating, creating a concentrated demand for grid power. Thermal storage therefore primarily shifts electricity use from high-price to low-price periods in this case; it does not reduce the maximum power demand over the entire day. In Figure 6b, the maximum grid power demand under CO on the typical day is approximately 7 MW, compared with peaks close to 10 MW under BS and FWO. Spare heat pump capacity allows heat to be stored in advance, reducing reliance on electric heating during the morning load increase. CO also permits discharge during the morning intermediate-price period, rather than requiring all stored heat to be retained until peak-price periods. This alleviates the concentrated grid power demand as the heating load rises. Although FWO achieves lower grid power demand during some peak-price hours, it retains the morning power peak, reflecting the timing restrictions imposed by its fixed discharge window. The contrast between the two operating

conditions shows that a reduction in maximum daily power depends on the load level and the heat source used for charging. Minimizing operating costs should not be equated with minimizing peak power demand.



(**a**) Extremely cold day (**b**) Typical day

Figure 6. Grid power demand under the three strategies.

5.3. Heating-Season Operating Costs

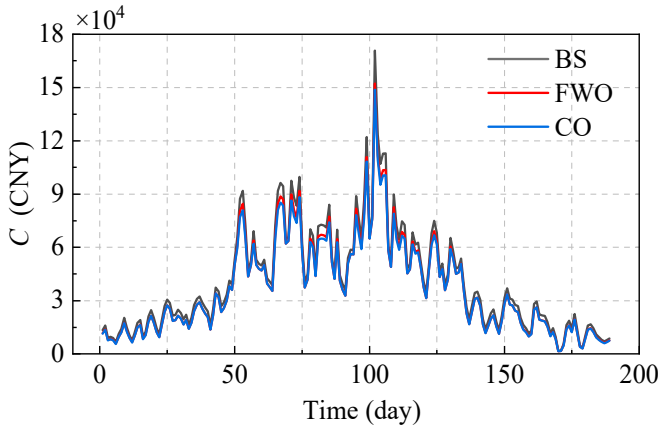
As reported in Table 6, FWO and CO reduce heating-season operating costs by 8.49% and 10.01%, respectively, relative to BS. Thermal storage scheduling therefore remains economically beneficial when evaluated over the heating season, and relaxing the charging and discharging windows provides additional savings. Relative to BS, CO reduces peak-period electricity purchases by 45.83% and the maximum grid power demand during peak-price periods by approximately 58.3%, while increasing total electricity purchases by 5.00%. The primary benefit is improved electricity-use timing, lower operating costs, and reduced electricity demand during high-price periods, rather than a substantial reduction in electricity consumption. The reduction in peak-period maximum power applies only to peak-price hours and should not be interpreted as a reduction in the maximum power demand across all hours of the day.

Table 6. Heating-season operating results.

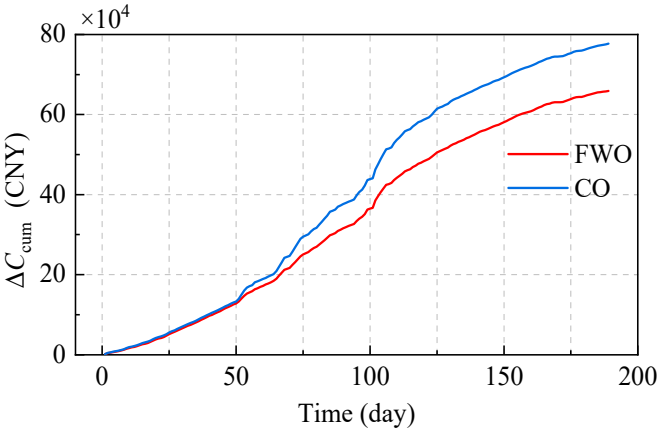
Strategy	Cost (10^4 CNY)	Cost Savings (%)	Total Electricity (MWh)	Peak-Period Electricity (MWh)	Peak-Period Maximum Power (MW)
BS	776.23	0.00	12,236.10	3741.53	25.637
FWO	710.31	8.49	12,935.06	1973.73	16.603
CO	698.55	10.01	12,847.68	2026.90	10.702

For the 800,000 m^2 case study, the 10.01% reduction corresponds to an absolute saving of CNY 0.7768 million per heating season, decreasing the operating cost from CNY 7.7623 million under BS to CNY 6.9855 million under CO. Compared with FWO, CO provides an additional saving of CNY 0.1176 million (1.66%). Together with the reductions in peak-period electricity purchases and peak-period maximum grid power, these operating-cost savings may justify the added scheduling layer when suitable BMS/PLC interfaces are already available. The reported operating costs include electricity purchase costs and variable O&M costs for the GSHP, electric heater, and thermal storage tank. Capital investment, control-system integration costs, fixed O&M costs, and the cost impacts of forecast errors are not included. An investment payback assessment therefore requires additional site-specific cost information.

Figure 7 traces daily cost and accumulated savings through the heating season. In Figure 7a, all three cost curves rise during the middle of the season and fall toward its ends. On high-load days, direct supply occupies more heat pump capacity and auxiliary electric heating contributes more heat. The cost gap between strategies changes accordingly, because both the heat available for storage and the cost of the heat it replaces vary with load. Storage benefits are therefore not a constant proportion of operating costs. In Figure 7b, cumulative savings increase more rapidly during the middle of the heating season and more slowly near its beginning and end, consistent with the daily cost differences shown in Figure 7a. Higher midseason heating demand provides more opportunities to displace high-cost heat production, yielding larger absolute daily savings. At the beginning and end of the season, more spare heat source capacity is available, but the amount of heat that can usefully be shifted is limited, and storage losses must still be compensated. Savings consequently accumulate more slowly. The cumulative savings gap between CO and FWO generally widens, showing that the additional benefits of flexible charging and discharging schedules accumulate over the heating season.



(**a**) Daily operating cost

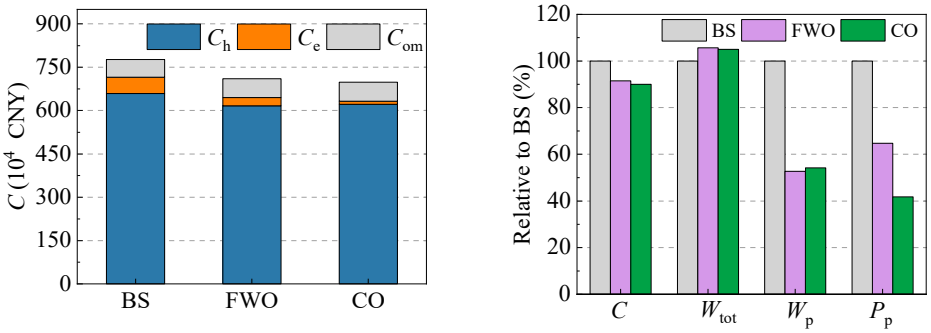


(**b**) Cumulative cost savings relative to BS

Figure 7. Heating-season operating costs and cumulative savings.

Figure 8 compares the cost breakdown and electricity-use indicators across strategies. In Figure 8a, heat pump electricity costs remain the largest component, consistent with the GSHP's role as the primary heat source. With thermal storage in operation, electric heater electricity costs decrease substantially because stored heat meets part of the demand otherwise supplied by direct electric heating during high-price periods, while some heat production is shifted to lower-price periods. Meanwhile, tank charging and discharging

throughput incurs additional operation and maintenance expenses, and changes in total heat production and its allocation among heat sources also affect O&M costs. The reduction in total operating costs is therefore the net result of lower electricity purchase costs and additional operation and maintenance expenses. A decrease in the electricity bill of an individual device does not, by itself, establish a reduction in its electricity consumption. In Figure 8b, operating costs and total electricity use change in opposite directions. The heat pump operates at a lower COP during charging than during direct heating, while charging and discharging losses and standby heat losses increase the heat production required to meet the same building demand. These effects raise the electricity requirement of the storage pathway. In this case study, the benefits of lower-cost heat production and the displacement of high-cost heat supply outweigh the costs of additional electricity consumption and operation and maintenance, allowing operating costs to fall while total electricity use increases. CO also purchases slightly more electricity during peak periods than FWO but incurs a lower operating cost, indicating that restricting all discharge to peak periods is not necessarily the most economical choice. Allowing stored heat to displace high-cost electric heating during intermediate-price periods can reduce full-day operating costs, even when some peak-period demand continues to be met by direct heat pump supply.



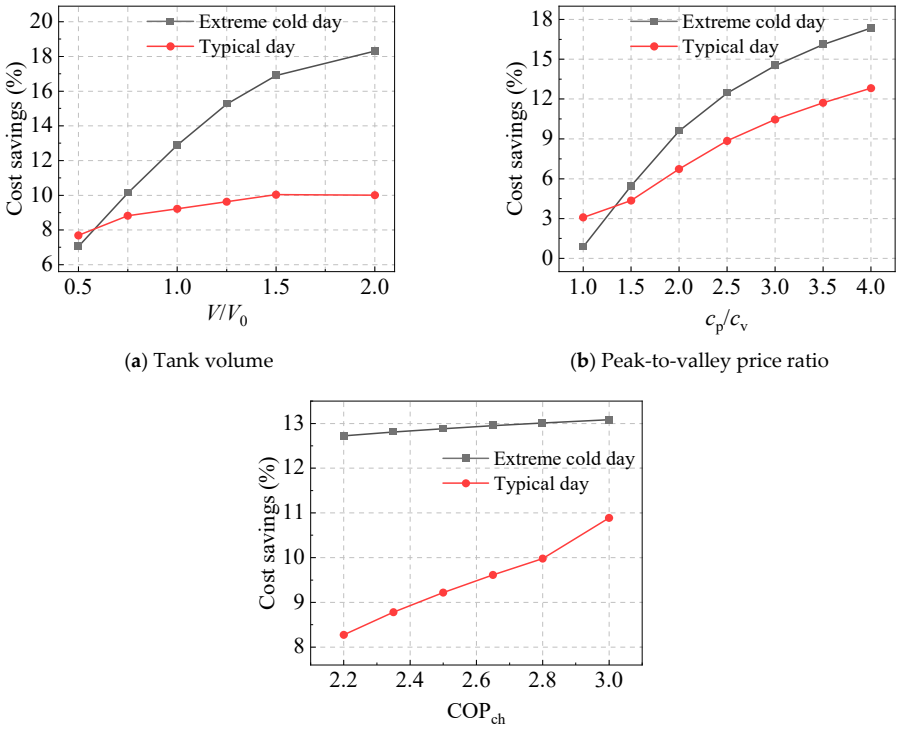
(**a**) Operating cost breakdown (**b**) Normalized performance indicators

Figure 8. Cost breakdown and normalized performance indicators.

5.4. Sensitivity Analysis

The tank volume, peak-to-valley electricity price ratio, and heat pump charging COP are varied individually to examine the sensitivity of the scheduling strategy to key parameters. Performance is evaluated using the percentage cost savings achieved by CO relative to BS, as shown in Figure 9.

In Figure 9a, the baseline tank volume is 2880 m^3, corresponding to a normalized tank volume of 1.0. The operating-cost savings of CO relative to BS increase with tank volume on the extremely cold day, although the marginal improvement diminishes. On the typical day, the operational benefits approach a plateau at approximately 1.5 times the baseline volume. A larger tank increases the amount of heat that can be shifted between periods, but additional capacity yields operating benefits only when sufficient charging capacity and subsequent heating demand are available. The greater reliance on auxiliary electric heating on the extremely cold day leaves considerable scope for displacing high-cost heat supply as storage capacity increases. On the typical day, utilization of the additional capacity becomes increasingly limited by spare heat source capacity, charging and discharging power limits, and the heating demand that can be displaced. The increase in the tank heat-loss coefficient accompanying enlargement may also offset some of the gains. This analysis is intended to evaluate the sensitivity of operating-cost savings to the tank volume under the fixed equipment configuration; it does not determine the optimal installed tank volume.



(**a**) Tank volume

(**b**) Peak-to-valley price ratio

(**c**) GSHP charging COP

Figure 9. Single-factor sensitivity analysis.

In Figure 9b, cost savings increase with the peak-to-valley price ratio under both operating conditions, with a more pronounced increase on the extremely cold day. With the intermediate-period price and the sum of the peak and off-peak prices held constant, increasing the ratio simultaneously lowers off-peak electricity purchase costs and raises the value of displacing peak-period heat supply. This strengthens the economic benefits of storage. Charging on the extremely cold day relies more heavily on electric heating, making its benefits more sensitive to the price difference between charging and discharging periods. At a peak-to-valley price ratio of 1, CO still saves money by using spare heat pump capacity during low-load hours to replace later electric heating. This route is economical when the heat pump's efficiency advantage covers tank losses and the additional operation and maintenance costs.

In Figure 9c, increasing the charging COP substantially improves cost savings on the typical day but produces only a modest improvement on the extremely cold day. This difference arises from the heat sources used for charging. On the typical day, the tank is charged mainly by the heat pump, so a higher COP directly reduces the electricity required to produce the same amount of heat for storage. On the extremely cold day, most heat pump capacity is allocated to direct heating, and tank charging relies more heavily on electric heating. Improvements in the heat pump charging COP therefore affect a smaller portion of system operation.

These sensitivity results show that CO retains a cost-saving advantage over BS within the tested ranges of tank volume, the peak-to-valley electricity price ratio, and the heat-pump charging COP, although the magnitude of the savings varies with operating conditions. Because the analysis uses one Daqing climate dataset, one tariff structure, and fixed COP values, the reported savings are case-specific. Their persistence under other realistic climates, tariff structures, and temperature-dependent COP conditions requires further multi-scenario analysis.

6. Conclusions

A MILP model was developed to coordinate a ground-source heat pump, an electric heater, and a thermal storage tank. The model was applied to office buildings in a severe cold region to evaluate scheduling performance over the heating season. The following conclusions are drawn:

(1) Thermal storage and coordinated scheduling reduce operating costs. Compared with the baseline strategy without storage, CO reduces heating-season operating costs by 10.01%. With the same storage configuration, CO also reduces costs by 1.66% relative to FWO. Removing predefined charging and discharging windows therefore provides additional economic benefits from operating flexibility.

(2) Effective storage scheduling depends on spare heat source capacity and the cost of the heat supply being displaced. On the extremely cold day, heat pump capacity is used mainly for direct heating, and tank charging relies more heavily on electric heating. On the typical day, spare heat pump capacity can be used to store heat in advance. CO allows stored heat to displace high-cost electric heating during intermediate-price periods, rather than requiring all stored heat to be retained until peak-price periods. This improves the economic value of the available stored heat.

(3) Relative to BS, CO reduces peak-period electricity purchases by 45.83% and the maximum grid power demand during peak-price periods by approximately 58.3%, while increasing total electricity purchases by 5.00%. The lower heat pump COP during charging compared with direct heating, together with storage losses, increases electricity requirements. Nevertheless, changes in electricity-use timing and the displacement of high-cost heat supply reduce operating costs. The strategy therefore primarily improves the timing of heat production and electricity use rather than substantially reducing electricity consumption.

(4) The benefits of parameter changes depend on operating conditions. Increasing tank volume expands the scope for shifting heat between periods but yields diminishing marginal returns. On the typical day, operational benefits approach a plateau at approximately 1.5 times the baseline volume. A higher peak-to-valley price ratio improves cost savings, whereas an increase in charging COP has a greater effect on the typical day, when charging is supplied mainly by the heat pump. Storage capacity should therefore be matched to heat source capabilities and load characteristics; the optimal size cannot be determined from operating cost savings alone.

For practical implementation, day-ahead heating demand forecasts, electricity tariffs, and available heat source capacity can guide storage scheduling. Charging should prioritize spare heat pump capacity during low-price periods. During extremely cold periods, supplementary electric charging should be considered only when the cost of stored heat, including storage losses, is lower than that of the heat supply it replaces. Discharging should target periods with higher avoidable heating costs, including intermediate-price periods, while ensuring that heating demand is met.

Author Contributions: L.Z. and S.G.: Validation, Writing—review and editing; C.Y.: Writing—original draft, Writing—review and editing, Methodology. All authors have read and agreed to the published version of the manuscript.

Funding: This study was supported by the Science and Technology Project of SPIC Engineering Company (No. 37-K2026-C088). The original contributions presented in this study are included in the article. Further inquiries can be directed to the corresponding author.

Data Availability Statement: The data supporting the findings of this study are available from the corresponding author upon reasonable request.

Conflicts of Interest: Long Zhang and Sujin Ge are employed by Shandong Electric Power Engineering Consulting Institute Co., Ltd. This research was funded by the Science and Technology Project of SPIC Engineering Company (Grant No. 37-K2026-C088). The funders had no role in the design of the study; in the collection, analyses, or interpretation of data; in the writing of the manuscript; or in the decision to publish the results. Cheng Yu declares no conflicts of interest.

References

1. Li, T.; Li, S.; Liang, X.; Wang, J. Techno-economic performance of air source heat pump and thermal energy storage considering peak-valley time-of-use electricity prices. *Clean. Energy Syst.* **2026**, *14*, 100274. [CrossRef]
2. Liu, R.; Liu, Z.; Chen, H.; Li, B.; Zhang, L. Optimal sizing and energy management strategy for an office building with photovoltaic, heat pump, thermal tank, and electric vehicle under time-of-use tariff. *Energy Convers. Manag.* **2024**, *314*, 118708. [CrossRef]
3. Zhang, S.; Zhang, L.; Zhang, X. Performance evaluation of existed ground source heat pump systems in buildings using auxiliary energy efficiency index: Cases study in Jiangsu, China. *Energy Build.* **2017**, *147*, 90–100. [CrossRef]
4. Kaneko, C.; Yoshinaga, M. Long-term operation analysis of a ground source heat pump with an air source heat pump as an auxiliary heat source in a warm region. *Energy Build.* **2023**, *289*, 113050. [CrossRef]
5. Zheng, Z.; Zhou, J.; Xu, F.; Zhang, R.; Deng, G. Integrated operation of PV assisted ground source heat pump and air source heat pump system: Performance analysis and economic optimization. *Energy Convers. Manag.* **2022**, *269*, 116091. [CrossRef]
6. Renaldi, R.; Kiprakis, A.; Friedrich, D. An optimisation framework for thermal energy storage integration in a residential heat pump heating system. *Appl. Energy* **2017**, *186*, 520–529. [CrossRef]
7. Arteconi, A.; Hewitt, N.J.; Polonara, F. Domestic demand-side management (DSM): Role of heat pumps and thermal energy storage (TES) systems. *Appl. Therm. Eng.* **2013**, *51*, 155–165. [CrossRef]
8. Teamah, H.M.; Lightstone, M.F. Numerical study of the electrical load shift capability of a ground source heat pump system with phase change thermal storage. *Energy Build.* **2019**, *199*, 235–246. [CrossRef]
9. Huang, C.; Wei, W.; Sun, Y.; Wang, W.; Li, Z.; Wang, S.; Deng, S. Energy saving and peak load shifting performance of tail water source heat pump integrated with large-scale thermal storage pool space heating system in technology park. *Energy Convers. Manag.* **2023**, *287*, 117032. [CrossRef]
10. Lyden, A.; Tuohy, P.G. Heat pump and thermal storage sizing with time-of-use electricity pricing. In *Proceedings of the 13th International Renewable Energy Storage Conference (IRES 2019), Düsseldorf, Germany, 12–14 March 2019*; Atlantis Press: Dordrecht, The Netherlands, 2019; Volume 4, pp. 29–40. [CrossRef]
11. Kim, D.W.; Heo, J. Economic and thermodynamic assessment of a thermal energy storage–based heat pump system under electricity pricing, government incentives, and operating temperature conditions. *J. Energy Storage* **2026**, *179*, 123836. [CrossRef]
12. Maier, L.; Schönegge, M.; Henn, S.; Hering, D.; Müller, D. Assessing mixed-integer-based heat pump modeling approaches for model predictive control applications in buildings. *Appl. Energy* **2022**, *326*, 119894. [CrossRef]
13. Liu, R.; Liu, Z.; Leng, Y.; Li, B.; Wu, Y. Economic model predictive control for an office building with photovoltaic, heat pump, thermal storage and electric vehicle under time-of-use tariff. *Build. Environ.* **2025**, *282*, 113312. [CrossRef]
14. Aguilera, J.J.; Padullés, R.; Meesenburg, W.; Markussen, W.B.; Zühlsdorf, B.; Elmegaard, B. Operation optimization in large-scale heat pump systems: A scheduling framework integrating digital twin modelling, demand forecasting, and MILP. *Appl. Energy* **2024**, *376*, 124259. [CrossRef]
15. Krützfeldt, H.; Vering, C.; Mehrfeld, P.; Müller, D. MILP design optimization of heat pump systems in German residential buildings. *Energy Build.* **2021**, *249*, 111204. [CrossRef]
16. Weeratunge, H.; Narsilio, G.; de Hoog, J.; Dunstall, S.; Halgamuge, S. Model predictive control for a solar assisted ground source heat pump system. *Energy* **2018**, *152*, 974–984. [CrossRef]
17. Finck, C.; Li, R.; Kramer, R.; Zeiler, W. Quantifying demand flexibility of power-to-heat and thermal energy storage in the control of building heating systems. *Appl. Energy* **2018**, *209*, 409–425. [CrossRef]
18. D'Ettorre, F.; Conti, P.; Schito, E.; Testi, D. Model predictive control of a hybrid heat pump system and impact of the prediction horizon on cost-saving potential and optimal storage capacity. *Appl. Therm. Eng.* **2019**, *148*, 524–535. [CrossRef]
19. Lyden, A.; Tuohy, P.G. Planning level sizing of heat pumps and hot water tanks incorporating model predictive control and future electricity tariffs. *Energy* **2022**, *238*, 121731. [CrossRef]
20. Thorsteinsson, S.; Kalaee, A.A.S.; Vogler-Finck, P.; Stærmose, H.L.; Katic, I.; Bendtsen, J.D. Long-term experimental study of price responsive predictive control in a real occupied single-family house with heat pump. *Appl. Energy* **2023**, *347*, 121398. [CrossRef]
21. Crawley, D.B.; Hand, J.W.; Kummert, M.; Griffith, B.T. Contrasting the capabilities of building energy performance simulation programs. *Build. Environ.* **2008**, *43*, 661–673. [CrossRef]

22. Buonomano, A.; Palombo, A. Building energy performance analysis by an in-house developed dynamic simulation code: An investigation for different case studies. *Appl. Energy* **2014**, *113*, 788–807. [CrossRef]
23. Jiang, H.; Li, H.; Du, R.; Yang, X.; Luo, X. Energy efficiency evaluation of operation modes for ground source heat pump coupled with phase change thermal storage heating system. *Appl. Therm. Eng.* **2026**, *298*, 131044. [CrossRef]

Disclaimer/Publisher's Note: The statements, opinions and data contained in all publications are solely those of the individual author(s) and contributor(s) and not of MDPI and/or the editor(s). MDPI and/or the editor(s) disclaim responsibility for any injury to people or property resulting from any ideas, methods, instructions or products referred to in the content.